# Effects of Channel-Estimation Errors on Receiver Selection-Combining Schemes for Alamouti MIMO Systems With BPSK

Wenyu Li, *Student Member, IEEE,* and Norman C. Beaulieu, *Fellow, IEEE*

*Abstract*—The bit-error rate (BER) of binary phase-shift keying in Rayleigh fading, using the Alamouti transmission scheme and receiver selection diversity in the presence of channel-estimation error, is studied. Closed-form expressions for the BER of log-likelihood ratio selection, signal-to-noise ratio (SNR) selection, switch-and-stay combining selection, and maximum ratio combining are derived in terms of the SNR and the cross-correlation coefficient of the channel gain and its corrupted estimate. Two new selection schemes, space–time sum-of-squares combining selection diversity and space–time sum-of-magnitudes selection diversity, are proposed and proven to provide almost the same performance as SNR selection, but with much simpler implementations. The effects of channel-estimation errors on each selection scheme are examined.

*Index Terms*—Alamouti multiple-input multiple-output (MIMO) systems, error analysis, estimation error, fading channels, pilot-symbol-assisted modulation (PSAM), selection diversity.

## I. INTRODUCTION

**M**ULTIPLE-INPUT multiple-output (MIMO) systems have attracted great interest, since they can improve the channel capacity and reliability of wireless communication [1]. However, adopting a MIMO system increases the system complexity and the cost of implementation. A promising approach for reducing implementation complexity, while retaining a reasonably good performance, is to employ some form of antenna selection.

In general, MIMO antenna selection combining (SC) includes receiver (Rx) antenna selection, transmitter (Tx) antenna selection, and joint Tx/Rx selection. Both Tx/Rx selection and Tx selection require that channel estimation be fed back from the Rx to the Tx. In order to avoid the need for a feedback channel, and to keep the system simple, some systems will implement Rx selection diversity only. In MIMO Rx selection diversity, $L_s$ out of $L$ Rx antennas are selected, while the Tx uses all available antennas. Some past work has examined MIMO Rx selection diversity. In [2]–[4], the Rx selection criteria are based on achieving the maximum received signal-to-noise ratio (SNR). An approximation of pairwise error probability is given in [2]. An upper bound on pairwise error probability is presented in [3]. In [4], an upper bound on bit-error rate (BER) is derived.

In this paper, we examine the effect of channel-estimation error on the BER performance of a MIMO system using binary phase-shift keying (BPSK) modulation and Rx selection diversity in a slow flat Rayleigh fading channel. The Alamouti space–time block code (STBC) [5] is used at the Tx. The "best" of $L$ Rx antennas is chosen according to some selection criterion. Since all SC schemes require some knowledge of the complex channel gains for all the diversity branches, and the complex channel gains have to be estimated at the Rx, channel-estimation errors affect the performance of all practical SC schemes. Quantitative results for the effects of noisy channel estimation are derived.

Five different selection schemes are considered for Rx antenna selection. The first scheme is log-likelihood ratio (LLR) selection, which was proposed in [6] for a one Tx antenna and $L$ Rx antennas system. In LLR selection, full knowledge of all the complex diversity branch gains is needed, and the branch providing the largest magnitude of LLR is chosen. This selection scheme was extended in [7] to include a two Tx antennas and $N_R$ Rx antennas system using the Alamouti scheme. The BER for this scheme is given by an expression involving a single integral. However, perfect channel estimation is assumed in [7]. Here, we derive a closed-form BER expression for this LLR selection scheme, accounting for the presence of channel-estimation errors.

Traditional SC is the second scheme considered in this paper. The selection of the best antenna is based on the largest SNR among the diversity branches at the detector input. Unlike LLR selection, which requires full knowledge of the complex channel gains for all the diversity branches, SNR selection only requires ordering fading amplitudes on the diversity branches. In [8], SNR selection is applied to Tx selection. Two Tx antennas which provide the largest and the second largest SNR are used for transmitting an STBC. The performance of the system is assessed in terms of an outage capacity analysis, but exact BER results are not given. In [4] and [7], the BER of SNR selection at the Rx side is evaluated. In this paper, this result is extended to include the effects of channel-estimation errors.

Since both LLR selection and SNR selection schemes require channel knowledge, we propose a new selection scheme, which we will refer to as space–time sum-of-squares (STSoS) selection. The STSoS selection scheme does not require knowledge of the channel gains to make the Rx antenna selection. Furthermore, branch selection is done before the space–time decoding, so that channel estimation for the space–time decoding is only performed for the branch selected, achieving a significant complexity reduction. Compared with the two former schemes, this new scheme is much simpler to implement. Significantly, it is shown in the following that it provides essentially the same performance as the SNR selection scheme.

The proposed STSoS SC scheme requires squaring the amplitudes of the received bit signals. In order to further simplify the hardware implementation, we propose another scheme, which only needs the amplitudes of the received bit signals. Similar to STSoS selection, this scheme, called space–time sum-of-magnitudes (STSoM) selection, does not require channel estimation. The simulation results in the following section show that STSoM selection has only slightly poorer BER performance than STSoS and SNR selection.

In order to implement all the former SC schemes, the Rx needs to monitor all the diversity branches to select the "best" branch. Furthermore, the Rx may switch frequently in order to use the best branches. It is desirable in some practical implementations to minimize switching in order to reduce switching transients. Therefore, SC is often implemented in the form of switched diversity [9], [10] in practical systems, in which rather than continuously picking the best branch, the Rx selects a particular branch until its SNR drops below a predetermined threshold. When this happens, the Rx switches to another branch. [11] and [12] investigate a switched diversity system with one Tx antenna and $N_R$ Rx antennas. A performance analysis for this system without space–time coding was given in Rayleigh fading in [11], and in Nakagami fading in [12]. In [13], switched diversity is applied at the Tx side and the cumulative distribution function (cdf), the probability density function (pdf), and the moment-generating function (MFG) of the received signal power are derived, again without space–time coding. In this paper, we analyze a transmission system with an Alamouti code at the Tx and switched diversity at the Rx. The average BER accounting for the effects of channel-estimation error is derived, and the optimal switching threshold that minimizes the BER for this switched diversity scheme is determined.

The remainder of this paper is organized as follows. In Section II, we present the system model. In Section III, we consider a wireless system with two Tx antennas using the Alamouti scheme and $L$ Rx antennas, and derive the BER for the four SC schemes with channel-estimation error considered. The analysis of a maximum ratio combining (MRC) Rx [14] is also recalled, and the performances of these four selection schemes are compared with the optimal MRC scheme. In Section IV, numerical results are presented and the relative performances of the four selection schemes are discussed. Conclusions are drawn in Section V.

## II. SYSTEM MODEL

In general, we consider a system where an Alamouti scheme [5] is applied with two Tx antennas and $L$ Rx antennas. Reference [5, Fig. 3] shows the STBC system for the special case of two Rx antennas for illustration. We assume a BPSK modulation, so that the transmitted signal is either $+1$ or $-1$. Signals $s_1$ and $s_2$, corresponding to two information bits, are sent simultaneously during two consecutive bit intervals. The corresponding

received signals in these two intervals on the $i$th branch can be expressed as [5]

$$r_{1,i} = g_{1,i}s_1 + g_{2,i}s_2 + n_{1,i} \tag{1a}$$
$$r_{2,i} = -g_{1,i}s_2 + g_{2,i}s_1 + n_{2,i} \tag{1b}$$

where $g_{j,i}$, $j = 1, 2$, $i = 1, \ldots, L$ is the complex gain between the $j$th Tx antenna and the $i$th Rx antenna, and $n_{j,i}$, $j = 1, 2$, $i = 1, \ldots, L$ represents additive channel noise. The variances of the real (or imaginary) components of $g_{j,i}$ and $n_{j,i}$ are denoted by $\sigma_g^2$ and $\sigma_n^2$, respectively. The average SNR of the received signal is defined here as $\bar{\gamma} = 2\sigma_g^2/\sigma_n^2$. The maximum-likelihood (ML) decoding of $s_1$ and $s_2$ is based on the combiner outputs [5]

$$y_{1,i} = \hat{g}_{1,i}^* r_{1,i} + \hat{g}_{2,i} r_{2,i}^* \tag{2a}$$
$$y_{2,i} = \hat{g}_{2,i}^* r_{1,i} - \hat{g}_{1,i} r_{2,i}^* \tag{2b}$$

where $\hat{g}_{j,i}$ is the estimate of $g_{j,i}$ with variance $\sigma_{\hat{g}}^2$, in the real and imaginary parts. The signal estimate is $\hat{s}_j = \text{sgn}(\Re(y_{j,i}))$, $j = 1, 2$, where $\text{sgn}(x) = \text{signum}(x)$ is defined in [15, p. xlv].

The complex channel gains $g_{j,i}$ are estimated at the Rx prior to fading compensation. We assume identical statistics for the independent diversity branches, and that the correlation between $g_{j,i}$ and its estimate $\hat{g}_{j,i}$ is the same on each branch. Extending the results in [16] to include the case when the variances of the channel gain and its estimate are unequal, we define

$$g_{j,i} = \left( \frac{R_c}{\sigma_{\hat{g}}^2} + j\frac{R_{cs}}{\sigma_{\hat{g}}^2} \right) \hat{g}_{j,i} + (x_{j,i} + jy_{j,i}) \tag{3}$$

where $x_{j,i}$ and $y_{j,i}$ are uncorrelated with $\hat{g}_{j,i}$. The parameters $R_c$ and $R_{cs}$ are given by

$$R_c = E[g_I \hat{g}_I] = E[g_Q \hat{g}_Q] \tag{4a}$$
$$R_{cs} = E[g_I \hat{g}_Q] = -E[g_Q \hat{g}_I]. \tag{4b}$$

Under the Rayleigh fading assumption, $R_{cs} = 0$ [17], and we can simplify (3) to

$$g_{j,i} = k\hat{g}_{j,i} + d_{j,i} \tag{5}$$

where $k = R_c/\sigma_{\hat{g}}^2$ and $d_{j,i} = (x_{j,i} + jy_{j,i})$. The variance of the real (or imaginary) component of $d_{j,i}$ is $\sigma_d^2 = (1 - \rho)\sigma_g^2$ [18], where $\rho$ is the squared amplitude of the cross-correlation coefficient of the channel fading and its estimate

$$\rho = \frac{E^2[g\hat{g}^*]}{E[|g|^2]E[|\hat{g}|^2]} = \frac{R_c^2}{\sigma_g^2 \sigma_{\hat{g}}^2} = \frac{\sigma_{\hat{g}}^2}{\sigma_g^2}k^2. \tag{6}$$

When pilot-symbol-assisted modulation (PSAM) is employed to estimate the fading channel gain, the cross-correlation coefficient of the channel fading and its estimate can be expressed as shown in (7) at the bottom of the page, where $K$ is the size of the interpolator, $h_k^n$ and $h_m^n$ are the interpolator coefficients, $f_D$ is the Doppler shift, $T_s$ is the symbol interval, $N$

$$\rho = \frac{\left[ \sum_{k=-\lfloor (K-1)/2 \rfloor}^{\lfloor K/2 \rfloor} h_k^n J_0(2\pi f_D |kN - 2n| T_s) \right]^2}{\sum_{k=-\lfloor (K-1)/2 \rfloor}^{\lfloor K/2 \rfloor} \sum_{m=-\lfloor (K-1)/2 \rfloor}^{\lfloor K/2 \rfloor} h_k^n h_m^n J_0(2\pi f_D |k - m| N T_s) + \frac{1}{\bar{\gamma}} \sum_{m=-\lfloor (K-1)/2 \rfloor}^{\lfloor K/2 \rfloor} (h_k^n)^2} \tag{7}$$

is the frame size, and $J_0(\cdot)$ is the zeroth-order Bessel function of the first kind. The detailed derivation of $\rho$ is in Appendix A.

## III. BIT-ERROR RATE ANALYSIS

By symmetry, the BER is the same for $s_1$ and $s_2$, so the following analysis will consider $s_1$ only. The results for $s_i, i = 1, 2$ can be obtained by appropriately renaming the variables.

Using (1), (2a), and (5), the combiner output $y_{1,i}$ can be written as

$$y_{1,i} = k\left(|\hat{g}_{1,i}|^2 + |\hat{g}_{2,i}|^2\right)s_1 + \left(\hat{g}_{1,i}^* d_{1,i} + \hat{g}_{2,i} d_{2,i}^*\right)s_1$$
$$+ \left(\hat{g}_{1,i}^* d_{2,i} - \hat{g}_{2,i} d_{1,i}^*\right)s_2 + \hat{g}_{1,i}^* n_{1,i} + \hat{g}_{2,i} n_{2,i}^*. \quad (8)$$

Since $s_2 = +s_1$ or $-s_1$, each with probability 1/2, we can calculate the BER as $P_b = 1/2(P_{b,s_2=s_1} + P_{b,s_2=-s_1}) = P_{b,s_2=s_1} = P_{b,s_2=s_1=1}$, where the last two equations follow from symmetry. For the case $s_2 = s_1 = 1$, from (8), we can write the decision variable for $y_{1,i}$ as

$$\Re(y_{1,i}) = k\left(|\hat{g}_{1,i}|^2 + |\hat{g}_{2,i}|^2\right)$$
$$+ \Re\left[\hat{g}_{1,i}^*(d_{1,i} + d_{2,i}) + \hat{g}_{2,i}(d_{2,i} - d_{1,i})^*\right]$$
$$+ \Re(\hat{g}_{1,i}^* n_{1,i}) + \Re(\hat{g}_{2,i} n_{2,i}^*). \quad (9)$$

Conditioning on $|\hat{g}_{1,i}|^2$ and $|\hat{g}_{2,i}|^2$, it can be shown that $\Re[\hat{g}_{1,i}^*(d_{1,i} + d_{2,i})]$, $\Re[\hat{g}_{2,i}^*(d_{2,i} - d_{1,i})]$, $\Re(\hat{g}_{1,i}^* n_{1,i})$ and $\Re(\hat{g}_{2,i} n_{2,i}^*)$ are independent, zero-mean Gaussian random variables with variance $2|\hat{g}_{1,i}|^2\sigma_d^2$, $2|\hat{g}_{2,i}|^2\sigma_d^2$, $|\hat{g}_{1,i}|^2\sigma_n^2$ and $|\hat{g}_{2,i}|^2\sigma_n^2$, respectively. Therefore, $\Re(y_{1,i})$, conditioned on $|\hat{g}_{1,i}|^2$ and $|\hat{g}_{2,i}|^2$, is a Gaussian random variable as well. It has mean $k(|\hat{g}_{1,i}|^2 + |\hat{g}_{2,i}|^2)$ and variance $(2\sigma_d^2 + \sigma_n^2)(|\hat{g}_{1,i}|^2 + |\hat{g}_{2,i}|^2)$.

To simplify the following BER calculation, we normalize the expression in (9) by dividing both sides of the equation with $2k\sigma_{\hat{g}}^2$. Then (9) can be written as

$$\Re(y_{1,i}') = \frac{\Re(y_{1,i})}{2k\sigma_{\hat{g}}^2}$$
$$= \frac{1}{2\sigma_{\hat{g}}^2}\left(|\hat{g}_{1,i}|^2 + |\hat{g}_{2,i}|^2\right)$$
$$+ \frac{1}{2k\sigma_{\hat{g}}^2}\left\{\Re\left[\hat{g}_{1,i}^*(d_{1,i} + d_{2,i}) + \hat{g}_{2,i}(d_{2,i} - d_{1,i})^*\right]\right.$$
$$\left. + \Re(\hat{g}_{1,i}^* n_{1,i}) + \Re(\hat{g}_{2,i} n_{2,i}^*)\right\}. \quad (10)$$

Let $a_i = (|\hat{g}_{1,i}|^2 + |\hat{g}_{2,i}|^2)/2\sigma_{\hat{g}}^2$; conditioned on $a_i$, the new decision variable $\Re(y_{1,i}')$ has mean $a_i$ and variance $((2\sigma_d^2 +$

$\sigma_n^2)/2k^2\sigma_{\hat{g}}^2)a_i$. Using (6) and $\sigma_d^2 = (1-\rho)\sigma_{\hat{g}}^2$, this variance is simplified to $(((1-\rho)\bar{\gamma}+1)/\rho\bar{\gamma})a_i$. Define the effective SNR

$$\bar{\gamma}_c = \frac{\rho\bar{\gamma}}{(1-\rho)\bar{\gamma} + 1}. \quad (11)$$

Then the variance is $a_i/\bar{\gamma}_c$.

Since $\hat{g}_{1,i}$ and $\hat{g}_{2,i}$ are independent, zero-mean complex Gaussian random variables, $a_i$ has a chi-square distribution with four degrees of freedom, and its pdf is given by [14]

$$f_A(a_i) = a_i \exp(-a_i). \quad (12)$$

### A. LLR SC

The LLR Rx selection system model is described in [7]. With the Alamouti scheme and imperfect channel estimation, the LLR for data $s_1$, given $\hat{g}_{j,i}, j = 1, 2$ and $y_{1,i}$ is

$$\Lambda_i = \ln\frac{P(s_1 = +1|\hat{g}_{j,i}, y_{1,i})}{P(s_1 - 1|\hat{g}_{j,i}, y_{1,i})} = \ln\frac{p(y_{1,i}|\hat{g}_{j,i}, s_1 = +1)}{p(y_{1,i}|\hat{g}_{j,i}, s_1 = -1)}. \quad (13)$$

From (8), conditioning on $\hat{g}_{j,i}$, we can show that $y_{1,i}$ is a complex Gaussian random variable with mean $k(|\hat{g}_{1,i}|^2 + |\hat{g}_{2,i}|^2)s_1 = m_y s_1$ and real/imaginary part variance $\sigma_y^2 = (2\sigma_d^2 + \sigma_n^2)(|\hat{g}_{1,i}|^2 + |\hat{g}_{2,i}|^2)$. Then continuing (13), we have

$$\Lambda_i = \ln\frac{\exp\left[\frac{-|y_{1,i} - m_y|^2}{(2\sigma_y^2)}\right]}{\exp\left[\frac{-|y_{1,i} + m_y|^2}{(2\sigma_y^2)}\right]} = \frac{2m_y}{\sigma_y^2}\Re(y_{1,i})$$
$$= \frac{2k}{(2\sigma_d^2 + \sigma_n^2)}\Re(y_{1,i}) = \frac{2R_c}{(2\sigma_d^2 + \sigma_n^2)\sigma_{\hat{g}}^2}\Re(y_{1,i}). \quad (14)$$

Since $R_c$, $\sigma_d^2$, $\sigma_n^2$, and $\sigma_{\hat{g}}^2$ are the same across all the Rx branches, the LLR Rx SC is equivalent to selecting the branch providing the largest amplitude of $\Re(y_{1,i})$. Note, with perfect channel estimation, i.e., when $R_c = \sigma_{\hat{g}}^2 = \sigma_g^2$ and $\sigma_d^2 = 0$, $\Lambda_i = (4/N_0)\Re(y_{1,i})$, which matches the result in [7, eq. (37)], where $N_0$ is the noise power spectral density.

The final expression for the BER is derived in Appendix B. It is shown in (15) at the bottom of the next page, where $A - C$ and $m_1-m_7$ are given in (39b) and (40b), respectively.

A simpler suboptimum SC rule was also proposed by Kim and Kim in [6]. Instead of the amplitude of $\Re(y_{1,i})$, $|(y_{1,i})|$ is used for this envelope-LLR SC. Simulation results for the BER of this envelope-LLR selection scheme will be given together with results for the other SC schemes in Section IV.

$$P_b = L\sum_{n=0}^{L-1}\sum_{m=0}^{L-1-n}\sum_{p=0}^{n}\sum_{q=0}^{m}\sum_{i=0}^{1}\binom{L-1}{n}\binom{L-1-n}{m}\binom{n}{p}\binom{m}{q}$$
$$\times AB^i m_1^{n-p}m_2^p m_4^{m-q}m_5^q m_7^{L-1-n-m}\frac{(-1)^{m+p}(p+q+i)!}{(m_3 n + m_6 m + B + C)^{p+q+i+1}} \quad (15)$$
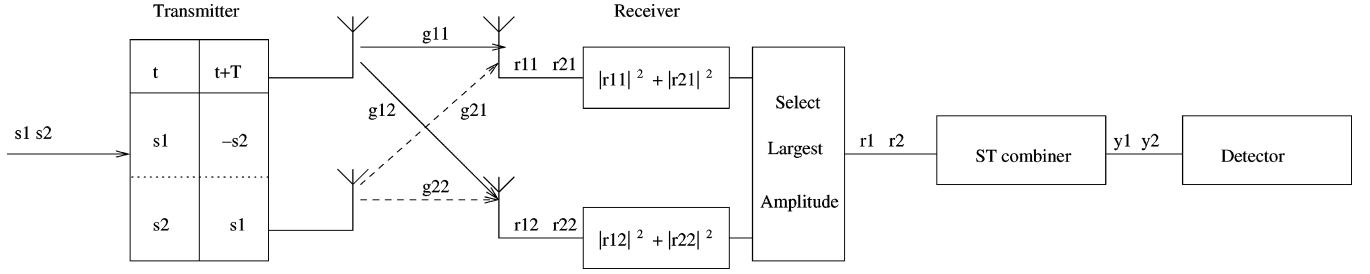
Fig. 1. STSoS Rx selection system model.

## B. SNR SC

The Rx SC scheme model is same as the model in [4] and [7]. In SNR SC, the Rx antenna with the largest SNR will be chosen for space–time decoding. From (8), the SNR, given the $i$th Rx antenna selected, is $k^2(|\hat{g}_{1,i}|^2+|\hat{g}_{2,i}|^2)/2(2\sigma_d^2+\sigma_n^2) = \bar{\gamma}_c a_i/2$. Therefore, the antenna providing the largest SNR is the one providing the largest $a_i$. Let $A_{\max} = \max[(|\hat{g}_{1,i}|^2+|\hat{g}_{2,i}|^2)/2\sigma_{\hat{g}}^2]$. Then, the expression of the BER can be rewritten as [7]

$$P_b = L \cdot \int_0^\infty \Pr\left(\Re(y_{1,i}) \leq 0 \,|\, A_{\max} = a\right) f_{A_{\max}}(a)\,da$$
$$= \int_0^\infty Q\left(\sqrt{\bar{\gamma}_c a}\right) f_{A_{\max}}(a)\,da \tag{16a}$$

where the pdf of $A_{\max}$ is [19]

$$f_{A_{\max}}(a) = L\left[\int_0^a f_A(a_i)\,da_i\right]^{L-1} f_A(a)$$
$$= L\left[1 - (1+a)\exp(-a)\right]^{L-1} f_A(a) \tag{16b}$$

and $f_A(a)$ is given in (12).

Expanding $\left[\int_0^a f_A(a)\,da\right]^{L-1}$ in (16) using the binomial theorem gives

$$P_b = L \times \sum_{i=0}^{L-1}\sum_{j=0}^{i}\binom{L-1}{i}\binom{i}{j}(-1)^i$$
$$\times \int_0^\infty Q\left(\sqrt{\bar{\gamma}_c a}\right) a^{j+1}\exp[-(i+1)a]\,da. \tag{17}$$

Integrating (17) term-by-term, the final expression for the BER is derived as

$$P_b = L \times \sum_{i=0}^{L-1}\sum_{j=0}^{i}\sum_{m=0}^{j+1}(-1)^i\binom{L-1}{i}\binom{i}{j}$$
$$\times \frac{(j+1+m)!}{m!(1+i)^{j+2}}\left(\frac{1-\mu_1}{2}\right)^{j+2}\left(\frac{1+\mu_1}{2}\right)^m \tag{18a}$$
$$\mu_1 = \sqrt{\frac{\bar{\gamma}_c}{\bar{\gamma}_c + 2i + 2}}. \tag{18b}$$

## C. New SC Method 1: STSoS Selection

Both LLR-based and SNR-based SC schemes require knowledge of all the Rx branch fading gains in order to decide which branch to choose. This increases the Rx complexity. Here, we propose a new selection-diversity scheme that selects the branch providing the largest sum of the squared amplitudes of the two received bit signals, i.e., $|r_{1,i}|^2+|r_{2,i}|^2$ (see Fig. 1). This scheme

is similar to square-law combining, although square-law combining is used for noncoherent modulation and we deal with coherent modulation here. To the best of the authors' knowledge, this SC diversity scheme as used in space–time coding here with coherent modulation is novel. We will call it STSoS selection. The advantage of this selection scheme is that it does not require channel estimation to perform the selection. Hence, the Rx implementation is simpler than other selection schemes. Moreover, this new scheme provides comparable performance to SNR-based selection, as is shown in Section IV.

The system model is shown in Fig. 1. Observe that

$$2|r_{1,i}|^2 + 2|r_{2,i}|^2$$
$$= |r_{1,i} + r_{2,i}|^2 + |r_{1,i} - r_{2,i}|^2$$
$$= |g_{1,i}(s_1 - s_2) + g_{2,i}(s_1 + s_2) + n_{1,i} + n_{2,i}|^2$$
$$+ |g_{1,i}(s_1 + s_2) + g_{2,i}(s_2 - s_1) + n_{1,i} - n_{2,i}|^2 \tag{19a}$$

and, observe further that $s_1 + s_2 = \pm 2$ and $s_1 - s_2 = 0$, or $s_1 + s_2 = 0$ and $s_2 - s_1 = \pm 2$, so that

$$|r_{1,i} + r_{2,i}|^2 + |r_{1,i} - r_{2,i}|^2$$
$$= \begin{cases} |\pm 2g_{1,i} + n_{1,i} + n_{2,i}|^2 + |\pm 2g_{2,i} + n_{1,i} - n_{2,i}|^2, & s_1 = -s_2 \\ |\pm 2g_{2,i} + n_{1,i} + n_{2,i}|^2 + |\pm 2g_{1,i} + n_{1,i} - n_{2,i}|^2, & s_1 = s_2. \end{cases} \tag{19b}$$

Thus, selecting the branch having the maximum value of $|r_{1,i}|^2 + |r_{2,i}|^2$ is equivalent to selecting the branch with the maximum value of

$$|g_{1,i} + n_1^e|^2 + |g_{2,i} + n_2^e|^2 \tag{20}$$

where $n_1^e$ and $n_2^e$ are independent, complex noise samples, each of variance $\sigma_n^2/2$ in each of the real and imaginary components. Note that when the SNR becomes large, STSoS selection is equivalent to selecting the branch with the maximum value of $|g_{1,i}|^2 + |g_{2,i}|^2$, because the noise terms in (20) become small. On the other hand, in SNR SC, selecting the antenna providing the largest $a_i = (|\hat{g}_{1,i}|^2 + |\hat{g}_{2,i}|^2)/2\sigma_{\hat{g}}^2$ is equivalent to selecting the antenna providing the largest $|\hat{g}_{1,i}|^2 + |\hat{g}_{2,i}|^2$, because the $\sigma_{\hat{g}}^2$ is the same over all the Rx branches. Since the channel gain estimate depends on the SNR, with a large SNR value, one has $\hat{g}_{j,i} \to g_{j,i}$, $j = 1, 2$. As a result, the SNR selection is equivalent to selecting the branch with the maximum value of $|g_{1,i}|^2 + |g_{2,i}|^2$ as well when the SNR becomes large, and STSoS selection becomes equivalent to SNR-based selection in slow fading. Observe further that the noise affecting the branch selection is effectively reduced by 3 dB in the STSoS combiner.
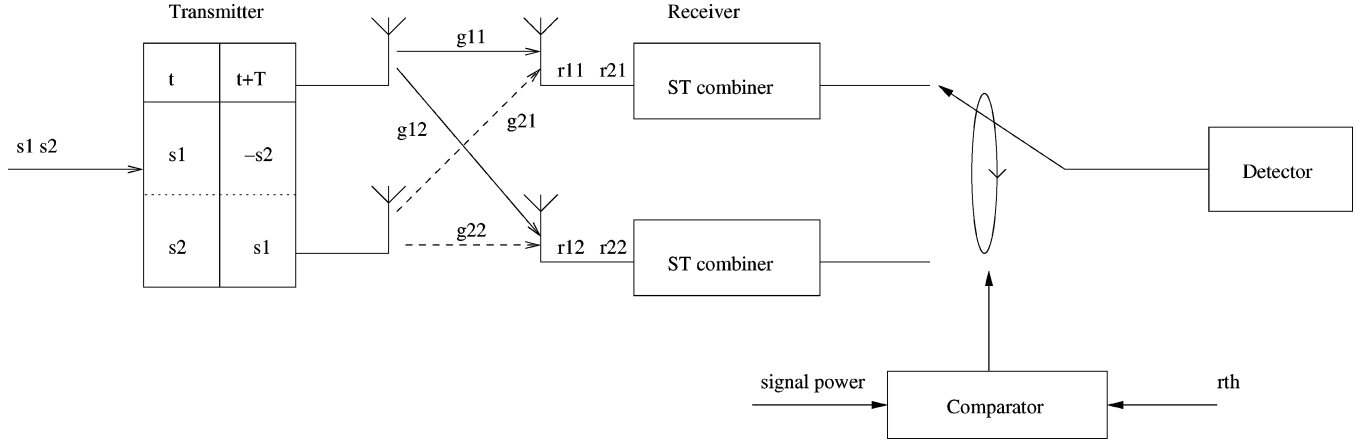
Fig. 2. SSC Rx selection system model.

Also note that when the SNR becomes small, both STSoS selection and SNR selection become dominated by noise terms, e.g., $n_j^e$, $j = 1, 2$ for STSoS selection and estimation error for SNR selection. Both these terms are Gaussian distributed, such that the BER performances of both selection methods approach 0.5. As a result, the BER difference between the two methods is indistinguishable.

The simulation results in the following section show that STSoS selection has essentially the same performance as SNR-based selection.

### D. New SC Method 2: STSoM Selection

The proposed STSoS SC scheme, which selects the branch providing the largest sum of $|r_{1,i}|^2 + |r_{2,i}|^2$, requires squaring the amplitudes of the received bit signals before making the selection. In order to further simplify the hardware implementation, we propose another scheme which selects the branch with the largest sum, $|r_{1,i}| + |r_{2,i}|$. Similar to STSoS selection, this scheme, called STSoM selection, does not require channel estimation. It is simpler than STSoS selection because the Rx only needs to obtain the amplitudes of the two received signals $r_{1,i}$ and $r_{2,i}$, and then take the sum. The simulation results in the following section show that it has only slightly poorer BER performance than STSoS and SNR selection.

### E. Switch-and-Stay Selection

Switch-and-stay SC (SSC) [11] functions in the following manner: assuming antenna 1 is being used, one switches to antenna 2 only if the instantaneous signal power in antenna 1 falls below a certain threshold, $\gamma_{\text{th}}$, regardless of the value of the instantaneous signal power in antenna 2. The switching from antenna 2 to antenna 1 is performed in the same manner. The system model is shown in Fig. 2. The major advantage of this strategy is that only one envelope signal need be examined at any instant. Therefore, it is much simpler to implement than traditional SC, because it is not necessary to keep track of the signals from both antennas simultaneously. However, the performance of SSC is poorer than the performance of SC. Using the Alamouti scheme at the Tx antenna side, and assuming the fadings on the Rx antenna branches are independent and identically Rayleigh distributed, the number of branches at the Rx

side does not affect the average BER performance [13]. Consequently, only the case of two Rx antennas is examined here.

In Rx SSC, with channel-estimation error, the BER is related to the instantaneous effective SNR of the selected $i$th branch $\gamma_c$ in (8), where $\gamma_c = k^2(|\hat{g}_{1,i}|^2 + |\hat{g}_{2,i}|^2)/2(2\sigma_d^2 + \sigma_n^2)$. Conditioning on the pdf of $\gamma_c$, the BER is $Q(\sqrt{2\gamma_c})$. The final BER expression is derived in Appendix C. It is

$$P_b = K_1 - \left[ K_1 \left( \frac{2\gamma_{th}}{\bar{\gamma}_c} + 1 \right) - \frac{2\gamma_{\text{th}} + \bar{\gamma}_c}{\bar{\gamma}_c} Q(\sqrt{2\gamma_{\text{th}}}) \right.$$
$$\left. + \frac{\sqrt{\gamma_{\text{th}}}}{\sqrt{\pi}(\bar{\gamma}_c + 2)} \exp(-\gamma_{\text{th}}) \right] \exp\left( -\frac{2\gamma_{\text{th}}}{\bar{\gamma}_c} \right)$$
$$- K_2 Q \left( \sqrt{\frac{2\gamma_{\text{th}}(\bar{\gamma}_c + 2)}{\bar{\gamma}_c}} \right) \tag{21}$$

where $K_1$ and $K_2$ are given in (45b).

Note that the BER depends on the value of the switching threshold $\gamma_{\text{th}}$. The optimal value, $\gamma_{\text{th}}^*$, is a solution of the equation $(\partial P_e / \partial \gamma_{\text{th}})|_{\gamma_{\text{th}} = \gamma_{\text{th}}^*} = 0$. Differentiating (21) with respect to $\gamma_{\text{th}}$, we get

$$\gamma_{\text{th}}^* = \frac{1}{2} \left[ Q^{-1}(\alpha) \right]^2, \alpha = \frac{1}{2} - \frac{\bar{\gamma}_c \sqrt{\bar{\gamma}_c}}{2\sqrt{(\bar{\gamma}_c + 2)^3}} - \frac{3\sqrt{\bar{\gamma}_c}}{2\sqrt{(\bar{\gamma}_c + 2)^3}} \tag{22}$$

where $Q^{-1}(\cdot)$ denotes the inverse Gaussian Q-function, and $\bar{\gamma}_c$ is the effective SNR (11).

### F. MRC Diversity

In MRC, all the combiner outputs are weighted and summed to form the decision variable as illustrated in [5, Fig. 1]. From (10), the combiner output is

$$\Re \left[ \sum_{i=1}^{L} y_{1,i}' \right] = \frac{1}{2\sigma_{\hat{g}}^2} \sum_{i=1}^{L} \left( |\hat{g}_{1i}|^2 + |\hat{g}_{2i}|^2 \right) + \frac{1}{2k\sigma_{\hat{g}}^2}$$
$$\cdot \Re \sum_{i=1}^{L} \left[ \hat{g}_{1,i}^*(d_{1,i} + d_{2,i}) \right.$$
$$\left. + \hat{g}_{2,i}(d_{2,i} - d_{1,i})^* + \hat{g}_{1,i}^* n_{1,i} + \hat{g}_{2,i} n_{2,i}^* \right]. \tag{23}$$

Fig. 3.   BER versus SNR for the 2 TX and 2 Rx system using an Alamouti STBC.
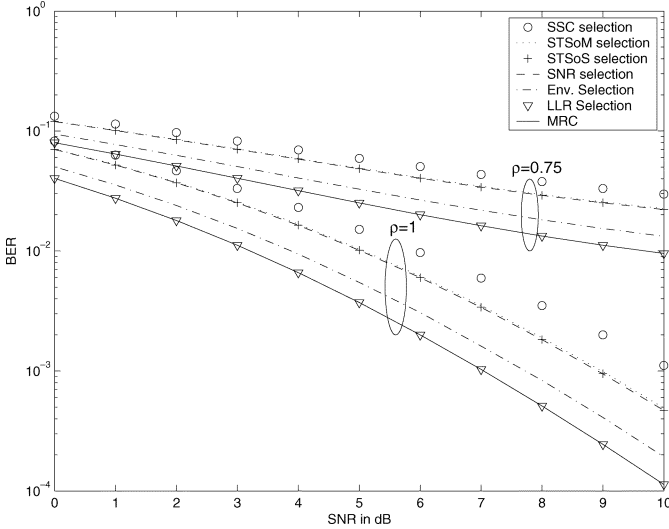


Fig. 4.   BER versus SNR for the 2 TX and 4 Rx system using an Alamouti STBC.

Conditioned on $y = \sum_{i=1}^{L}(|\hat{g}_{1i}|^2 + |\hat{g}_{2i}|^2)/2\sigma_{\hat{g}}^2$, this decision variable is a Gaussian random variable with mean $y$ and variance $y/\bar{\gamma}_c$. The pdf of $y$ is chi-square distributed with $4L$ degrees of freedom [14]

$$f_Y(y) = \frac{1}{(2L-1)!}y^{2L-1}\exp(-y). \qquad (24)$$

Following [14], the BER for MRC with Alamouti coding is obtained as

$$P_b = \int_0^\infty Q\left(\sqrt{\bar{\gamma}_c y}\right)f_Y(y)dy \qquad (25a)$$

$$= \left[\frac{1}{2}(1-\mu_2)\right]^{2L}\sum_{k=0}^{2L-1}\binom{2L-1+k}{k}\left[\frac{1}{2}(1+\mu_2)\right]^k$$

$$\mu_2 = \sqrt{\frac{\bar{\gamma}_c}{\bar{\gamma}_c + 2}}. \qquad (25b)$$

## IV. NUMERICAL RESULTS AND DISCUSSION

The BER results in this paper are functions of $\bar{\gamma}_c$, which is, in turn, a function of $\rho$ and $\bar{\gamma}$. Figs. 3 and 4 show plots of the average BER versus SNR per bit for the different selection-diversity schemes in a flat Rayleigh fading channel with perfect channel estimation and cross-correlation 0.75, respectively. The envelope-LLR selection, STSoS selection, and STSoM selection schemes are evaluated by computer simulation. As expected, these results show that in all cases, the BER increases with increasing fading estimation error (decreasing value of $\rho$).

It is observed in Fig. 3 that the performances of LLR selection and MRC are the same for dual diversity. The performances are, indeed, identical, because for MRC, the sign of the combiner output $\Re(y_{1,1}) + \Re(y_{1,2})$ is determined by the maximum of $|\Re(y_{1,i})|$, which coincides with the LLR selection rule. It is also observed in Fig. 3 that the performances of STSoS selection and SNR selection are the same, at least to graphical accuracy.
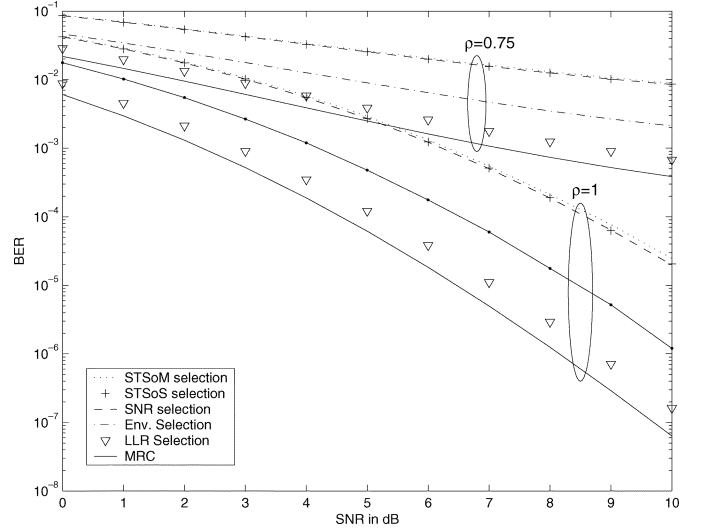
The STSoM selection scheme performs almost as well as the STSoS and SNR selection schemes, although it is simpler than both to implement. As does STSoS selection, STSoM selection choses the best branch without requiring any channel estimation. The envelope-LLR selection scheme, which does require channel estimation of all the channels, performs better than the STSoS, STSoM, and SNR selection schemes, but not as well as the LLR and MRC designs. The SSC selection offers the poorest performance, in exchange for its simplicity, as expected.

Fig. 4 shows the average BER as a function of SNR per bit for the various selection schemes used in four-fold diversity with perfect channel estimation and $\rho = 0.75$, respectively. There are a number of interesting observations. First, MRC and LLR are not the same, and MRC outperforms LLR, as expected. Second, the LLR selection outperforms envelope-LLR selection. Third, the envelope-LLR selection outperforms STSoS and STSoM. Fourth, the performances of SNR and STSoS selection are the same, as they were for the dual-branch case. This is a significant result. In order to implement SNR selection, the gains of all the diversity channels must be estimated. No channel estimation is required to implement STSoS selection. The demodulation will require channel estimation according to (2a), but in the case of STSoS, only two channel gains need to be estimated, while in the case of SNR selection, $2L$ channel gains must be estimated to implement the branch selection. We have also compared SNR and STSoS schemes for $L = 8$ and $L = 12$ [20]. In all cases, the performances are graphically the same.[1]

Figs. 5 and 6 show the average BER as a function of $\rho$ for the various selection schemes with a SNR of 5 dB per bit for dual diversity and four-fold diversity, respectively. Observe from both figures that with poor channel estimation, i.e., $\rho \to 0$, all the BER curves converge to 0.5. At this point, the system is only affected by random noise and offers the worst BER performance. With the increase of $\rho$, there is a decrease of error rate for all the selection schemes. When $\rho = 1$, systems with various selection

---

[1]Extended simulation tests indicate that the STSoS scheme outperforms SNR selection in the fourth or higher significant figure.
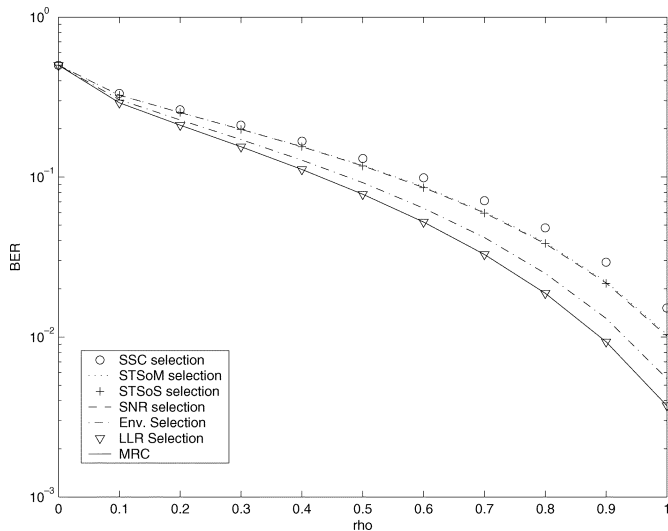
Fig. 5. BER versus $\rho$ for the 2 TX and 2 Rx system using an Alamouti STBC with $\bar{\gamma}_b = 5$ dB.
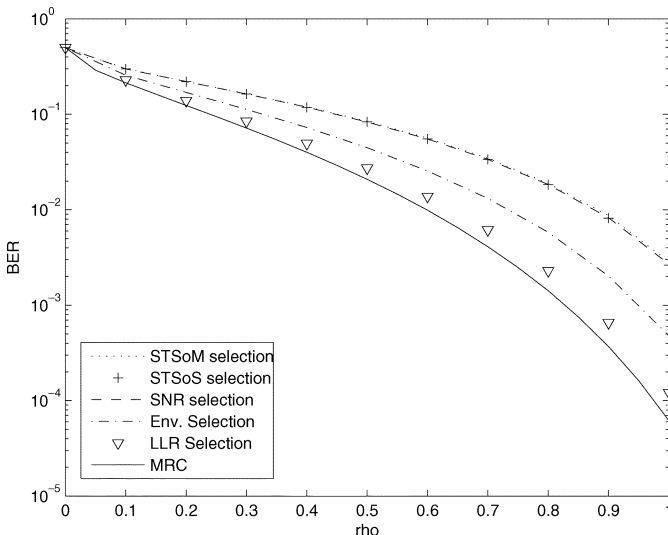


Fig. 6. BER versus $\rho$ for the 2 TX and 4 Rx system using an Alamouti STBC with $\bar{\gamma}_b = 5$ dB.

schemes reach the best performance, where the BER values match the values in Figs. 3 and 4 at the $\rho = 1$ and $\bar{\gamma}_b = 5$ dB point.

Figs. 3–6 show the average BER versus SNR for specific, constant values of $\rho$. These results show clearly the performance differences between the selection schemes. They are also representative of a situation where the Rx electronics has reached a limit, and cannot provide a better estimate of the channel gain. On the the other hand, many practical estimators will show a dependence on SNR, i.e., give better estimates as the SNR increases. In these cases, a larger SNR value leads to a better channel estimate, which means a higher value of $\rho$. To show this effect on BER, we consider PSAM as an example. We assume that a sinc interpolator with a Hamming window is used to interpolate fading estimates, with a frame size of 14, and normalized Doppler shift of 0.01.[2] Fig. 7 shows the average BER versus SNR from 0 to 10 dB with $L = 2$. Since $\rho$ is also a function of the symbol location, we give

[2]To simplify the analysis in this example, it is assumed that no branch switching occurs during a PSAM interpolation length. In the alternative, one can buffer the pilot symbols before the selection.
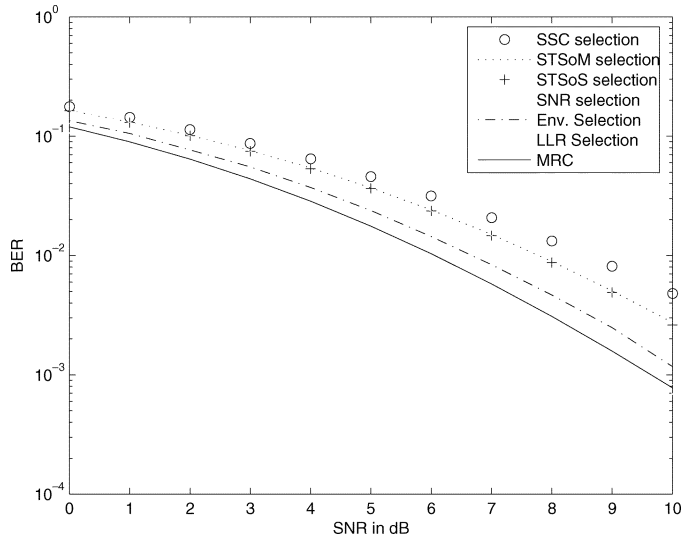


Fig. 7. PSAM BER versus SNR for the 2 TX and 2 Rx, STBC with Hamming windowing applied to a sinc interpolator for $K = 6$, $N = 14$, and $f_D T_s = 0.01$ with symbol location at $n = 3$.
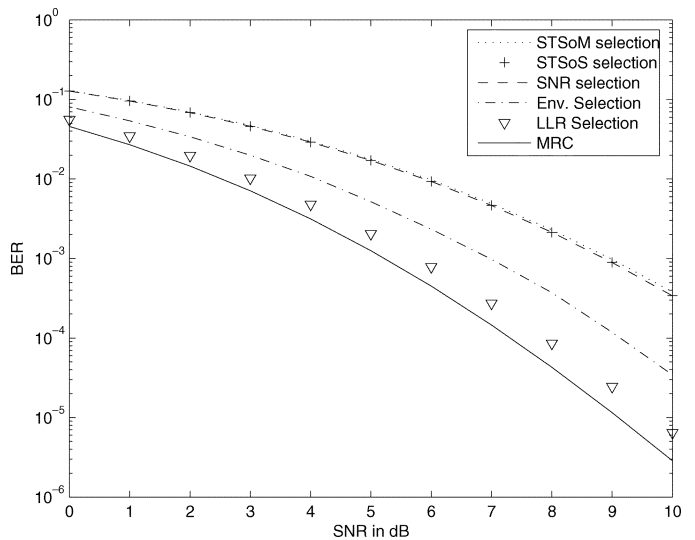


Fig. 8. PSAM BER versus SNR for the 2 TX and 4 Rx, STBC with Hamming windowing applied to a sinc interpolator for $K = 6$, $N = 14$, and $f_D T_s = 0.01$ with symbol location at $n = 3$.

the BER of the third data symbol in a frame as an example. Computed from (33), the value of $\rho$ for this PSAM system varies from 0.575 to 0.931 as the SNR varies from 0 to 10 dB. Similar to the results in Figs. 3 and 4, in Fig. 7, MRC and LLR selection still have the best performance, then envelope-LLR selection outperforms SNR and STSoS selection, which, in turn, slightly outperform STSoM selection. The simplest selection scheme, SSC selection, has the worst BER performance. Again, the performance of the SNR and STSoS schemes are indistinguishable. Fig. 8 shows similar results for four-fold diversity. In this case, MRC outperforms LLR selection, but SNR and STSoS selection again have the same performance, which is marginally better than STSoM selection.

## V. Conclusion

Analytical BER results were derived for LLR selection, SNR selection, SSC, and MRC with channel-estimation errors using Alamouti transmission systems. A new selection scheme,

STSoS selection, was proposed, with a much simpler hardware implementation. The results show that it has the same performance as SNR selection. A suboptimal selection scheme, STSoM, was also proposed with a still simpler implementation, but only slightly poorer performance than STSoS SC.

<div align="center">

APPENDIX A

DERIVATION OF $\rho$

</div>

### A. Fading Estimation in PSAM

We assume that PSAM is used for channel estimation. The PSAM frame format is similar to that considered in [21, Fig. 2], where pilot symbols are inserted periodically into the data sequence. Since there are two Tx antennas and an Alamouti scheme is employed, we consider two consecutive pilot symbols are transmitted together between data symbols. Under the assumption that the fading gain remains constant over two consecutive symbol intervals, $N/2$ clusters, each with two symbols, are formatted into one frame of $N$ symbols, where $N$ is an even number, with the first two pilot symbols ($n = 0$) followed by $N - 2$ data symbols ($1 \leq n \leq N/2 - 1$). The composite signal is transmitted over $2L$ flat, Rayleigh fading channels. At the Rx, after matched-filter detection, the pilot symbols are extracted and interpolated to form an estimate of the channel in the following manner.

Rewrite (1) to include the above assumptions as

$$r_{1,i,k}^n = g_{1,i,k}^n s_{1,i,k}^n + g_{2,i,k}^n s_{2,i,k}^n + n_{1,i,k}^n \qquad (26a)$$

$$r_{2,i,k}^n = -g_{1,i,k}^n s_{2,i,k}^n + g_{2,i,k}^n s_{1,i,k}^n + n_{2,i,k}^n \qquad (26b)$$

where $r_{1,i,k}^n$ denotes the first received symbol at the $n$th symbol cluster of the $k$th data frame in the $i$th Rx branch, and similarly for the fading gain $g$ and noise $n$. Since the pilot symbols are known to the Rx, without loss of generality, we assume that the two pilot symbols at the first cluster ($n = 0$) of the frame have the values $+1$ and $-1$, respectively. Then for the two received pilot symbols, (26a) becomes

$$r_{1,i,k}^0 = g_{1,i,k}^0 - g_{2,i,k}^0 + n_{1,i,k}^0 \qquad (27a)$$

$$r_{2,i,k}^0 = g_{1,i,k}^0 + g_{2,i,k}^0 + n_{2,i,k}^0. \qquad (27b)$$

Adding (27a) and (27b), we obtain the estimate of $g_{1,i,k}^0$ as

$$\hat{g}_{1,i,k}^0 = g_{1,i,k}^0 + \frac{n_{1,i,k}^0 + n_{2,i,k}^0}{2}. \qquad (28a)$$

Subtracting (27a) from (27b) generates

$$\hat{g}_{2,i,k}^0 = g_{2,i,k}^0 + \frac{n_{2,i,k}^0 - n_{1,i,k}^0}{2}. \qquad (28b)$$

The fading at the $n$th symbol ($1 \leq n \leq N/2 - 1$) in the $k$th frame of the $i$th branch is estimated from $2K$ pilot symbols of $K$ adjacent frames, with pilot symbols from $k_1 = -\lfloor (K-1)/2 \rfloor$ previous frames and to $k_2 = \lfloor K/2 \rfloor$ subsequent frames. These estimates are given by

$$\hat{g}_{1,i,k}^n = \sum_{k=-k_1}^{k_2} h_k^n \hat{g}_{1,i,k}^0 = \sum_{k=-k_1}^{k_2} h_k^n \left( g_{1,i,k}^0 + \frac{n_{1,i,k}^0 + n_{2,i,k}^0}{2} \right) \quad (29a)$$

$$\hat{g}_{2,i,k}^n = \sum_{k=-k_1}^{k_2} h_k^n \hat{g}_{2,i,k}^0 = \sum_{k=-k_1}^{k_2} h_k^n \left( g_{2,i,k}^0 + \frac{n_{2,i,k}^0 - n_{1,i,k}^0}{2} \right),$$

$$n = 1, \ldots \frac{N}{2} - 1 \qquad (29b)$$

where $h_k^n$ is the interpolation coefficient for the $n$th data symbol in the $k$th frame.

### B. Derivation of $R_c$

In an omnidirectional scattering Rayleigh fading channel, the autocorrelation of the real part of the fading gain is [21]

$$R(\tau) = \sigma_g^2 J_0(2\pi f_D \tau). \qquad (30)$$

Since calculation of the correlations for the data symbols is the same at all branches, we drop the subscripts $\{1, i\}$ and $\{2, i\}$ in (28), (29). Then, combining (28), (29) with (4a), (30), we have

$$R_c = E\left[g_{Ik}^n \hat{g}_{Ik}^n\right] = \sum_{k=-k_1}^{k_2} h_k^n E\left[g_{Ik}^n \left(g_{Ik}^0 + \frac{n_{1,k}^0 + n_{2,k}^0}{2}\right)\right]$$

$$= \sum_{k=-k_1}^{k_2} \sigma_g^2 h_k^n J_0(2\pi f_D |kN - 2n| T_s). \qquad (31)$$

### C. Derivation of $\sigma_{\hat{g}}^2$

From (28) and (29), the variance of $\hat{g}$ can be derived as

$$\sigma_{\hat{g}}^2 = \frac{1}{2} E\left[\hat{g}_k^n \hat{g}_k^{n*}\right] = \frac{1}{2} E\left[ \sum_{k=-k_1}^{k_2} h_k^n \left( g_{1,i,k}^0 + \frac{n_{1,i,k}^0 + n_{2,i,k}^0}{2} \right) \right.$$

$$\left. \times \sum_{k=-k_1}^{k_2} h_k^n \left( g_{1,i,k}^{0,*} + \frac{n_{1,i,k}^{0,*} + n_{2,i,k}^{0,*}}{2} \right) \right]$$

$$= \sum_{k=-k_1}^{k_2} \sum_{m=-k_1}^{k_2} h_k^n h_m^n \sigma_g^2 J_0(2\pi f_D |k-m| N T_s)$$

$$+ \frac{\sigma_n^2}{2} \sum_{m=-k_1}^{k_2} (h_k^n)^2. \qquad (32)$$

### D. Derivation of $\rho$

From (6), using (31) and (32), we have

$$\rho = \frac{R_c^2}{\sigma_g^2 \sigma_{\hat{g}}^2}$$

$$= \frac{\left[ \sum\limits_{k=-k_1}^{k_2} h_k^n J_0(2\pi f_D |kN - 2n| T_s) \right]^2}{\sum\limits_{k=-k_1}^{k_2} \sum\limits_{m=-k_1}^{k_2} h_k^n h_m^n J_0(2\pi f_D |k-m| N T_s) + \frac{1}{\gamma} \sum\limits_{m=-k_1}^{k_2} (h_k^n)^2}. \qquad (33)$$

Note that $\rho$ is a function of the type of interpolator, the data symbol location, the Doppler shift, the data frame length, and the symbol interval. When a sinc interpolator [22] is used and a Hamming window is applied, the interpolation coefficients are given by

$$h_k^n = \mathrm{sinc}\left(\frac{2n}{N} - k\right)$$

$$\times \left[0.54 - 0.46 \cos\left(\frac{2\pi(2n - kN)}{KN - 1} + \frac{2\pi \lfloor \frac{KN}{2} \rfloor}{KN - 1}\right)\right]. \qquad (34)$$

## APPENDIX B
### DERIVATION OF (15)

Similar to the analysis in [23], the BER for LLR Rx SC is

$$P_b = \sum_{i=1}^{L} \Pr(\Re(y_{1,i}) < 0, i\text{th branch selected}). \qquad (35)$$

Since $\Re(y_{1,i})$ is proportional to $\Re(y'_{1,i})$, conditioning $\Re(y'_{1,i})$ in (10) on $\hat{g}_{1,i}$ and $\hat{g}_{2,i}$ yields

$$
\begin{aligned}
P_b &= \sum_{i=1}^{L} \Pr(\Re(y'_{1,i}) < 0, i\text{th branch selected}) \\
&= L \cdot \Pr\left(\Re(y'_{1,1}) < 0, 1\text{th branch selected}\right) \\
&= L \cdot \Pr\left(\Re(y'_{1,1}) < 0, \left|\Re(y'_{1,1})\right| > \left|\Re(y'_{1,i})\right|_{\forall i, i \neq 1}\right) \\
&= L \cdot \Pr\left(-\Re(y'_{1,1}) > \left|\Re(y'_{1,i})\right|_{\forall i, i \neq 1}\right).
\end{aligned}
\qquad (36)
$$

Let $r_i = \Re(y'_{1,i})$ and $r_1 = -\Re(y'_{1,1})$, then

$$
\begin{aligned}
P_b & \\
=\,& L \int_0^\infty \Pr\left(\left|r_i = \Re(y'_{1,i})\right|_{\forall i, i \neq 1} < r_1 \Big| r_1 = -\Re(y'_{1,1})\right) f_R(r_1) dr_1 \\
=\,& L \int_0^\infty [\Pr(-r_1 < r_i < r_1 | r_1)]^{L-1} f_R(r_1) dr_1
\end{aligned}
\qquad (37)
$$

where $f_R(r_1)$ is the pdf of $r_1$. Since $r_1 = -\Re(y'_{1,1})$, $f_R(r_1)$ is equal to $f_{r_i}(-r_1)$, where $f_{r_i}(x)$ is the pdf of $r_i$. From (10), one has that $\Re(y'_{1,i})_{\forall i, i \neq 1}$ is Gaussian distributed with mean $a_i$ and variance $a_i/\bar{\gamma}_c$, when conditioned on $a_i = (|\hat{g}_{1,i}|^2 + |\hat{g}_{2,i}|^2)/2\sigma_{\hat{g}}^2$. Averaging over $a_i$, the pdf of $r_i$ is given by

$$
\begin{aligned}
f_{r_i}(x) &= \int_0^\infty f_{r_i}(x|a_i) f_A(a_i) da_i \\
&= \int_0^\infty \sqrt{\frac{\bar{\gamma}_c}{2\pi a_i}} \exp\left[-\frac{\bar{\gamma}_c(x - a_i)^2}{2a_i}\right] a_i \exp(-a_i) da_i.
\end{aligned}
\qquad (38)
$$

Changing the variable of integration to $z = \sqrt{a_i}$, and using the result from [15, eq. (3.472)]

$$
\begin{aligned}
\int_0^\infty b^2 \exp\left(-c_1 \frac{1}{b^2} - c_2 b^2\right) db \\
= \frac{1}{4}\sqrt{\frac{\pi}{c_2^3}}(1 + 2\sqrt{c_1 c_2}) \exp(-2\sqrt{c_1 c_2})
\end{aligned}
$$

(38) can be simplified as

$$f_{r_i}(x) = A(1 + B|x|)\exp(-B|x| + Cx) \qquad (39a)$$

where $\quad A = \dfrac{\sqrt{\bar{\gamma}_c(\bar{\gamma}_c + 2)}}{(\bar{\gamma}_c + 2)^2} \quad B = \sqrt{\bar{\gamma}_c(\bar{\gamma}_c + 2)} \quad C = \bar{\gamma}_c. \qquad (39b)$

Then, for the $i$th branch

$$
\begin{aligned}
\Pr(-r_1 < r_i < r_1 | r_1) &= \int_{-r_1}^{r_1} f_{r_i}(x) dx \\
&= m_7 + (m_1 - m_2 r_1)\exp(-m_3 r_1) \\
&\quad - (m_4 + m_5 r_1)\exp(-m_6 r_1)
\end{aligned}
\qquad (40a)
$$

$$
\begin{aligned}
\text{where} \quad & m_1 = \frac{AC - 2AB}{(C - B)^2} \quad m_2 = \frac{AB}{B - C} \\
& m_3 = B - C \quad m_4 = \frac{2AB + AC}{(B + C)^2} \\
& m_5 = \frac{AB}{B + C} \quad m_6 = B + C \quad m_7 = \frac{4AB^3}{(B^2 - C^2)^2}.
\end{aligned}
\qquad (40b)
$$

Combining (37), (38), and (40), the final expression for the BER is obtained as (41), shown at the bottom of the page.

## APPENDIX C
### DERIVATION OF (21)

Following [12], the cdf of $\gamma_c$ can be written as

$$
F(\gamma_c) = \begin{cases} \Pr(\gamma_{c,1} \leq \gamma_c)\Pr(\gamma_{c,2} \leq \gamma_{\text{th}}), & \text{if } \gamma_c < \gamma_{\text{th}} \\ \Pr(\gamma_{\text{th}} \leq \gamma_{c,1} \leq \gamma_c) + \Pr(\gamma_{c,1} \leq \gamma_c) \\ \quad \Pr(\gamma_{c,2} \leq \gamma_{\text{th}}), & \text{if } \gamma_c \geq \gamma_{\text{th}}. \end{cases}
\qquad (42)
$$

From (12), both $\gamma_{c,1}$ and $\gamma_{c,2}$ have a chi-squared distribution given by

$$f(\gamma_{c,i}) = \frac{4\gamma_{c,i}}{\bar{\gamma}_c^2}\exp\left(-\frac{2\gamma_{c,i}}{\bar{\gamma}_c}\right), \quad i = 1,2. \qquad (43)$$

The pdf is obtained by differentiating the cdf in (42) with respect to $\gamma_c$

$$
f(\gamma_c) = \begin{cases} \left[1 - \left(\frac{2\gamma_{\text{th}}}{\bar{\gamma}_c} + 1\right)\exp\left(-\frac{2\gamma_{\text{th}}}{\bar{\gamma}_c}\right)\right]\frac{4\gamma_c}{\bar{\gamma}_c^2}\exp\left(-\frac{2\gamma_c}{\bar{\gamma}_c}\right), & \gamma_c < \gamma_{\text{th}} \\ \left[2 - \left(\frac{2\gamma_{\text{th}}}{\bar{\gamma}_c} + 1\right)\exp\left(-\frac{2\gamma_{\text{th}}}{\bar{\gamma}_c}\right)\right]\frac{4\gamma_c}{\bar{\gamma}_c^2}\exp\left(-\frac{2\gamma_c}{\bar{\gamma}_c}\right), & \gamma_c \geq \gamma_{\text{th}}. \end{cases}
\qquad (44)
$$

$$
\begin{aligned}
P_b =\,& L \int_0^\infty [m_7 + (m_1 - m_2 r_1)\exp(-m_3 r_1) - (m_4 + m_5 r_1)\exp(-m_6 r_1)]^{L-1} \times A(1 + Br_1)\exp(-Br_1 - Cr_1) dr_1 \\
=\,& L \sum_{n=0}^{L-1}\sum_{m=0}^{L-1-n}\sum_{p=0}^{n}\sum_{q=0}^{m}\sum_{i=0}^{1}\binom{L-1}{n}\binom{L-1-n}{m}\binom{n}{p}\binom{m}{q} \times AB^i m_1^{n-p} m_2^p m_4^{m-q} m_5^q m_7^{L-1-n-m}\frac{(-1)^{m+p}(p+q+i)!}{(m_3 n + m_6 m + B + C)^{p+q+i+1}}
\end{aligned}
\qquad (41)
$$

Then, the BER is

$$P_b = \int_0^\infty Q\left(\sqrt{2\gamma_c}\right) f(\gamma_c) d\gamma_c$$

$$= K_3 \int_0^\infty Q(\sqrt{2\gamma_c}) \frac{4\gamma_c}{\bar{\gamma}_c^2} \exp\left(-\frac{2\gamma_c}{\bar{\gamma}_c}\right) d\gamma_c$$

$$+ \int_{\gamma_{th}}^\infty Q(\sqrt{2\gamma_c}) \frac{4\gamma_c}{\bar{\gamma}_c^2} \exp\left(-\frac{2\gamma_c}{\bar{\gamma}_c}\right) d\gamma_c$$

$$= K_1 - \left[ K_1\left(\frac{2\gamma_{th}}{\bar{\gamma}_c} + 1\right) - \frac{2\gamma_{th} + \bar{\gamma}_c}{\bar{\gamma}_c} Q(\sqrt{2\gamma_{th}}) \right.$$

$$\left. + \frac{\sqrt{\gamma_{th}}}{\sqrt{\pi}(\bar{\gamma}_c + 2)} \exp(-\gamma_{th}) \right] \exp\left(-\frac{2\gamma_{th}}{\bar{\gamma}_c}\right)$$

$$- K_2 Q\left(\sqrt{\frac{2\gamma_{th}(\bar{\gamma}_c + 2)}{\bar{\gamma}_c}}\right) \qquad (45a)$$

where $K_1 = \dfrac{\sqrt{(\bar{\gamma}_c + 2)^3} - \bar{\gamma}_c \sqrt{\bar{\gamma}_c} - 3\sqrt{\bar{\gamma}_c}}{2\sqrt{(\bar{\gamma}_c + 2)^3}}$

$$K_2 = \frac{\bar{\gamma}_c + 3}{\bar{\gamma}_c + 2} \sqrt{\frac{\bar{\gamma}_c}{\bar{\gamma}_c + 2}}$$

$$K_3 = 1 - \left(\frac{2\gamma_{th}}{\bar{\gamma}_c} + 1\right) \exp\left(-\frac{2\gamma_{th}}{\bar{\gamma}_c}\right). \qquad (45b)$$

## REFERENCES

[1] G. Foschini and M. Gans, "On the limits of wireless communications in a fading environment when using multiple antennas," *Wireless Pers. Commun.*, vol. 6, no. 3, pp. 311–335, Mar. 1998.

[2] A. Ghrayeb and T. M. Duman, "Performance analysis of MIMO systems with antenna selection over quasi-static fading channels," *IEEE Trans. Veh. Technol.*, vol. 52, no. 2, pp. 281–288, Mar. 2003.

[3] I. Bahceci, T. M. Duman, and Y. Altunbasak, "Antenna selection for multiple-antenna transmission systems: Performance analysis and code construction," *IEEE Trans. Inf. Theory*, vol. 49, no. 10, pp. 2669–2681, Oct. 2003.

[4] X. Zeng and A. Ghrayeb, "Performance bounds for space–time block codes with receive antenna selection," *IEEE Trans. Inf. Theory*, vol. 50, no. 9, pp. 2130–2137, Sep. 2004.

[5] S. M. Alamouti, "A simple transmit diversity technique for wireless communications," *IEEE J. Sel. Areas Commun.*, vol. 16, no. 10, pp. 1451–1458, Oct. 1998.

[6] S. W. Kim and E. Y. Kim, "Optimum selection diversity for BPSK signals in Rayleigh fading channels," *IEEE Trans. Commun.*, vol. 49, no. 10, pp. 1715–1718, Oct. 2001.

[7] ——, "Optimum receive antenna selection minimizing error probability," in *Proc. Wireless Commun. Netw. Conf.*, vol. 1, Mar. 2003, pp. 441–447.

[8] D. Gore and A. Paulraj, "Space–time block coding with optimal antenna selection," in *Proc. IEEE Int. Conf. Acoust., Speech, Signal Process.*, vol. 4, May 2001, pp. 2441–2444.

[9] W. C. Jakes, *Microwave Mobile Communications*. Piscataway, NJ: IEEE Press, 1993.

[10] W. Lee, *Mobile Communications Engineering*. New York: McGraw-Hill, 1982.

[11] M. A. Blanco and K. J. Zdunek, "Performance and optimization of switched diversity systems for the detection of signals with Rayleigh fading," *IEEE Trans. Commun.*, vol. COM-27, no. 12, pp. 1887–1895, Dec. 1979.

[12] A. A. Abu-Dayya and N. C. Beaulieu, "Analysis of switched diversity systems on generalized-fading channels," *IEEE Trans. Commun.*, vol. 42, no. 11, pp. 2959–2966, Nov. 1994.

[13] H. Yang and M. Alouini, "Performance analysis of multibranch switched diversity systems," *IEEE Trans. Commun.*, vol. 51, no. 5, pp. 782–794, May 2003.

[14] J. G. Proakis, *Digital Communications*. New York: McGraw-Hill, 1995.

[15] I. S. Gradshteyn and I. M. Ryzhik, *Table of Integral, Series, and Products*, 6th ed, A. Jeffrey and D. Zwillinger, Eds. New York: Academic, 2000.

[16] M. J. Gans, "The effect of Gaussian error in maximal ratio combiners," *IEEE Trans. Commun. Technol.*, vol. COM-19, no. 8, pp. 492–500, Aug. 1971.

[17] G. L. Stüber, *Principles of Mobile Communication*, 2nd ed. Norwell, MA: Kluwer, 2001.

[18] L. Cao and N. C. Beaulieu, "Exact error-rate analysis of diversity 16-QAM with channel estimation error," *IEEE Trans. Commun.*, vol. 52, no. 6, pp. 1019–1029, Jun. 2004.

[19] H. A. David, *Order Statistics*. New York: Wiley, 1981.

[20] W. Li, "Effects of channel estimation errors on receiver selection combining diversity for Alamouti MIMO systems," M.S. thesis, Univ. Alberta, Edmonton, AB, Canada, 2005.

[21] J. K. Cavers, "An analysis of pilot symbol assisted modulation for Rayleigh fading channels," *IEEE Trans. Veh. Technol.*, vol. 40, no. 6, pp. 686–693, Nov. 1991.

[22] Y.-S. Kim, C.-J. Kim, G.-Y. Jeong, Y.-J. Bang, H.-K. Park, and S. S. Choi, "New Rayleigh fading channel estimator based on PSAM channel sounding technique," in *Proc. IEEE Int. Conf. Commun.*, vol. 3, Jun. 1997, pp. 1518–1520.

[23] E. A. Neasmith and N. C. Beaulieu, "New results on selection diversity," *IEEE Trans. Commun.*, vol. 46, no. 5, pp. 695–703, May 1998.

**Wenyu Li** received the B.S.E.E. degree from Shanghai Jiaotong University, Shanghai, China, in 1993, and the M.S.E.E. degree from the University of Alberta, Edmonton, AB, Canada in 2005.

She was employed with China Telecom, Zhuhai, China, as a Telecommunications Engineer from July 1993 to August 1999, specializing in telephone network management and optimization. Her current research interests are in the area of wireless communications, with a focus on diversity, antenna selection, channel estimation, and space–time coding.
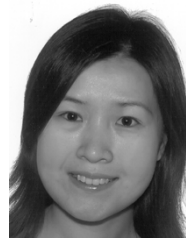
**Norman C. Beaulieu** (S'82–M'86–SM'89–F'99) received the B.A.Sc. (honors), M.A.Sc., and Ph.D. degrees in electrical engineering from the University of British Columbia, Vancouver, BC, Canada, in 1980, 1983, and 1986, respectively.

He was a Queen's National Scholar Assistant Professor with the Department of Electrical Engineering, Queen's University, Kingston, ON, Canada, from September 1986 to June 1988, an Associate Professor from July 1988 to June 1993, and a Professor from July 1993 to August 2000. In September 2000, he became the *i*CORE Research Chair in Broadband Wireless Communications at the University of Alberta, Edmonton, AB, Canada, and in January 2001, the Canada Research Chair in Broadband Wireless Communications. His current research interests include broadband digital communications systems, fading channel modeling and simulation, interference prediction and cancellation, decision-feedback equalization, and space–time coding.

Dr. Beaulieu is a Member of the IEEE Communication Theory Committee and served as its Representative to the Technical Program Committee of the 1991 International Conference on Communications and as Co-Representative to the Technical Program Committee of the 1993 International Conference on Communications and the 1996 International Conference on Communications. He was General Chair of the Sixth Communication Theory Mini-Conference in association with GLOBECOM '97 and Co-Chair of the Canadian Workshop on Information Theory 1999. He has been an Editor for Wireless Communication Theory of the IEEE TRANSACTIONS ON COMMUNICATIONS since January 1992, and was Editor-in-Chief from January 2000 to December 2003. He served as an Associate Editor for Wireless Communication Theory of the IEEE COMMUNICATIONS LETTERS from November 1996 to August 2003. He has also served on the Editorial Board of the PROCEEDINGS OF THE IEEE since November 2000. He received the Natural Science and Engineering Research Council of Canada (NSERC) E. W. R. Steacie Memorial Fellowship in 1999. He was awarded the University of British Columbia Special University Prize in Applied Science in 1980 as the highest standing graduate in the faculty of Applied Science. He is a Fellow of The Royal Society of Canada.